07-11 July 2011

TECH BRIEFS

NATIONAL AERONAUTICS AND SPACE ADMINISTRATION

- Technology Focus
- Electronics/Computers
- Software
- Materials
- Mechanics/Machinery
- Manufacturing
- Bio-Medical
- Physical Sciences
- Information Sciences
- Books and Reports
- Green Design

INTRODUCTION

Tech Briefs are short announcements of innovations originating from research and development activities of the National Aeronautics and Space Administration. They emphasize information considered likely to be transferable across industrial, regional, or disciplinary lines and are issued to encourage commercial application.

Additional Information on NASA Tech Briefs and TSPs

Additional information announced herein may be obtained from the NASA Technical Reports Server: **http://ntrs.nasa.gov**.

Please reference the control numbers appearing at the end of each Tech Brief. Information on NASA's Innovative Partnerships Program (IPP), its documents, and services is available on the World Wide Web at **http://www..ipp.nasa.gov**.

Innovative Partnerships Offices are located at NASA field centers to provide technology-transfer access to industrial users. Inquiries can be made by contacting NASA field centers listed below.

NASA Field Centers and Program Offices

Ames Research Center
Mary Walsh
(650) 604-1405
mary.w.walsh@nasa.gov

Dryden Flight Research Center
Ron Young
(661) 276-3741
ronald.m.young@nasa.gov

Glenn Research Center
Joe Shaw
(216) 977-7135
robert.j.shaw@nasa.gov

Goddard Space Flight Center
Nona Cheeks
(301) 286-5810
nona.k.cheeks@nasa.gov

Jet Propulsion Laboratory
Indrani Graczyk
(818) 354-2241
indrani.graczyk@jpl.nasa.gov

Johnson Space Center
John E. James
(281) 483-3809
john.e.james@nasa.gov

Kennedy Space Center
David R. Makufka
(321) 867-6227
david.r.makufka@nasa.gov

Langley Research Center
Michelle Ferebee
(757) 864-5617
michelle.t.ferebee@nasa.gov

Marshall Space Flight Center
Jim Dowdy
(256) 544-7604
jim.dowdy@nasa.gov

Stennis Space Center
Ramona Travis
(228) 688-3832
ramona.e.travis@ssc.nasa.gov

NASA Headquarters

Innovative Partnerships Office
Doug Comstock, Director
(202) 358-2221
doug.comstock@nasa.gov

Daniel Lockney,
Technology Transfer Lead
(202) 358-2037
daniel.p.lockney@nasa.gov

Small Business Innovation Research (SBIR) & Small Business Technology Transfer (STTR) Programs
Carl Ray, Program Executive
(202) 358-4652
carl.g.ray@nasa.gov

NASA TECH BRIEFS

NATIONAL AERONAUTICS AND SPACE ADMINISTRATION

5 Technology Focus: Sensor
5 Collaborative Clustering for Sensor Networks
5 Teleoperated Marsupial Mobile Sensor Platform Pair for Telepresence Insertion Into Challenging Structures
6 Automated Verification of Spatial Resolution in Remotely Sensed Imagery
6 Electrical Connector Mechanical Seating Sensor
7 *In Situ* Aerosol Detector
7 Multi-Parameter Aerosol Scattering Sensor

9 Electronics/Computers
9 MOSFET Switching Circuit Protects Shape Memory Alloy Actuators
9 Optimized FPGA Implementation of Multi-Rate FIR Filters Through Thread Decomposition
10 Circuit for Communication Over Power Lines
10 High-Efficiency Ka-Band Waveguide Two-Way Asymmetric Power Combiner
11 10–100 Gbps Offload NIC for WAN, NLR, and Grid Computing
11 Pulsed Laser System to Simulate Effects of Cosmic Rays in Semiconductor Devices

13 Software
13 Flight Planning in the Cloud
13 MPS Editor
13 Object-Oriented Multidisciplinary Design, Analysis, and Optimization Tool

15 Manufacturing & Prototyping
15 Cryogenic-Compatible Winchester Connector Mount and Retaining System for Composite Tubes
15 Development of Position-Sensitive Magnetic Calorimeters for X-Ray Astronomy

17 Mechanics/Machinery
17 Planar Rotary Piezoelectric Motor Using Ultrasonic Horns
17 Self-Rupturing Hermetic Valve
18 Explosive Bolt Dual-Initiated From One Side
18 Two-Stage Winch for Kites and Tethered Balloons or Blimps
18 Dampers for Stationary Labyrinth Seals
19 Two-Arm Flexible Thermal Strap

21 Green Design
21 Carbon Dioxide Removal via Passive Thermal Approaches
21 Polymer Electrolyte-Based Ambient Temperature Oxygen Microsensors for Environmental Monitoring
22 Pressure Shell Approach to Integrated Environmental Protection

23 Physical Sciences
23 Image Quality Indicator for Infrared Inspections
23 Micro-Slit Collimators for X-Ray/Gamma-Ray Imaging
23 Scatterometer-Calibrated Stability Verification Method
24 Test Port for Fiber-Optic-Coupled Laser Altimeter
25 Phase Retrieval System for Assessing Diamond Turning and Optical Surface Defects
25 Laser Oscillator Incorporating a Wedged Polarization Rotator and a Porro Prism as Cavity Mirror

27 Information Sciences
27 Generic, Extensible, Configurable Push-Pull Framework for Large-Scale Science Missions
27 Dynamic Loads Generation for Multi-Point Vibration Excitation Problems
28 Optimal Control Via Self-Generated Stochasticity
28 Space-Time Localization of Plasma Turbulence Using Multiple Spacecraft Radio Links
29 Surface Contact Model for Comets and Asteroids

31 Books & Reports
31 Dust Mitigation Vehicle
31 Optical Coating Performance for Heat Reflectors of the JWST-ISIM Electronic Component
31 SpaceCube Demonstration Platform
31 Aperture Mask for Unambiguous Parity Determination in Long Wavelength Imagers
32 Spaceflight Ka-Band High-Rate Radiation-Hard Modulator
32 Enabling Disabled Persons To Gain Access to Digital Medial

33 Bio-Medical
33 Cytometer on a Chip
33 Principles, Techniques, and Applications of Tissue Microfluidics

Collaborative Clustering for Sensor Networks

This technique can be used in sensor networks such as those for volcano and earthquake monitoring, intruder detection, target tracking, and data mining in cell phone networks.

NASA's Jet Propulsion Laboratory, Pasadena, California

Traditionally, nodes in a sensor network simply collect data and then pass it on to a centralized node that archives, distributes, and possibly analyzes the data. However, analysis at the individual nodes could enable faster detection of anomalies or other interesting events, as well as faster responses such as sending out alerts or increasing the data collection rate. There is an additional opportunity for increased performance if individual nodes can communicate directly with their neighbors.

Previously, a method was developed by which machine learning classification algorithms could collaborate to achieve high performance autonomously (without requiring human intervention). This method worked for supervised learning algorithms, in which labeled data is used to train models. The learners collaborated by exchanging labels describing the data. The new advance enables clustering algorithms, which do not use labeled data, to also collaborate. This is achieved by defining a new language for collaboration that uses pair-wise constraints to encode useful information for other learners. These constraints specify that two items must, or cannot, be placed into the same cluster. Previous work has shown that clustering with these constraints (in isolation) already improves performance.

In the problem formulation, each learner resides at a different node in the sensor network and makes observations (collects data) independently of the other learners. Each learner clusters its data and then selects a pair of items about which it is uncertain and uses them to query its neighbors. The resulting feedback (a "must" and "cannot" constraint from each neighbor) is combined by the learner into a consensus constraint, and it then re-clusters its data while incorporating the new constraint. A strategy was also proposed for "cleaning" the resulting constraint sets, which may contain conflicting constraints; this improves performance significantly. This approach has been applied to collaborative clustering of seismic and infrasonic data collected by the Mount Erebus Volcano Observatory in Antarctica.

Previous approaches to distributed clustering cannot readily be applied in a sensor network setting, because they assume that each node has the same "view" of the data set. A view is the set of features used to represent each object. When a single data set is partitioned across several computational nodes, distributed clustering works; all objects have the same view. But when the data is collected from different locations, using different sensors, a more flexible approach is needed. This approach instead operates in situations where the data collected at each node has a different view (e.g., seismic vs. infrasonic sensors), but they observe the same events. This enables them to exchange information about the likely cluster membership relations between objects, even if they do not use the same features to represent the objects.

This work was done by Kiri L. Wagstaff of Caltech, Jillian Green of California State University of Los Angeles, and Terran Lane of University of New Mexico for NASA's Jet Propulsion Laboratory. For more information, contact iaoffice@jpl.nasa.gov. NPO-47491

Teleoperated Marsupial Mobile Sensor Platform Pair for Telepresence Insertion Into Challenging Structures

This configuration adds more flexibility to robotic rescue operations.

John H. Glenn Research Center, Cleveland, Ohio

A platform has been developed for two or more vehicles with one or more residing within the other (a marsupial pair). This configuration consists of a large, versatile robot that is carrying a smaller, more specialized autonomous operating robot(s) and/or mobile repeaters for extended transmission. The larger vehicle, which is equipped with a ramp and/or a robotic arm, is used to operate over a more challenging topography than the smaller one(s) that may have a more limited inspection area to traverse. The intended use of this concept is to facilitate the insertion of a small video camera and sensor platform into a difficult entry area. In a terrestrial application, this may be a bus or a subway car with narrow aisles or steep stairs.

The first field-tested configuration is a tracked vehicle bearing a rigid ramp of fixed length and width. A smaller six-wheeled vehicle approximately 10 in. (25 cm) wide by 12 in. (30 cm) long resides at the end of the ramp within the larger vehicle. The ramp extends from the larger vehicle and is tipped up into the air. Using video feedback from a camera atop the larger robot, the operator at a remote location can steer the larger vehicle to the bus door. Once positioned at the door, the operator can switch video feedback to a camera at the end of the ramp to facilitate the mating of the end of the ramp to the top landing at the upper terminus of the steps. The ramp can be lowered by remote control until its end is in contact with the top landing. At the same time, the end of the ramp bearing the smaller vehicle is raised to minimize the angle of the slope the smaller vehicle has to climb, and fur-

ther gives the operator a better view of the entry to the bus from the smaller vehicle. Control is passed over to the smaller vehicle and, using video feedback from the camera, it is driven up the ramp, turned oblique into the bus, and then sent down the aisle for surveillance.

The demonstrated vehicle was used to scale the steps leading to the interior of a bus whose landing is 44 in. (≈1.1 m) from the road surface. This vehicle can position the end of its ramp to a surface over 50 in. (≈1.3 m) above ground level and can drive over rail heights exceeding 6 in. (≈15 cm). Thus configured, this vehicle can conceivably deliver the smaller robot to the end platform of New York City subway cars from between the rails. This innovation is scalable to other formulations for size, mobility, and surveillance functions. Conceivably the larger vehicle can be configured to traverse unstable rubble and debris to transport a smaller search and rescue vehicle as close as possible to the scene of a disaster such as a collapsed building. The smaller vehicle, tethered or otherwise, and capable of penetrating and traversing within the confined spaces in the collapsed structure, can transport imaging and other sensors to look for victims or other targets.

This work was done by Michael J. Krasowski, Norman F. Prokop, and Lawrence C. Greer of Glenn Research Center. Further information is contained in a TSP (see page 1).

Inquiries concerning rights for the commercial use of this invention should be addressed to NASA Glenn Research Center, Innovative Partnerships Office, Attn: Steven Fedor, Mail Stop 4–8, 21000 Brookpark Road, Cleveland, Ohio 44135. Refer to LEW-18673-1.

Automated Verification of Spatial Resolution in Remotely Sensed Imagery

Automated tool assesses image spatial resolution without the need for dedicated edge targets.

Stennis Space Center, Mississippi

Image spatial resolution characteristics can vary widely among sources. In the case of aerial-based imaging systems, the image spatial resolution characteristics can even vary between acquisitions. In these systems, aircraft altitude, speed, and sensor look angle all affect image spatial resolution. Image spatial resolution needs to be verified with estimators that include the ground sample distance (GSD), the modulation transfer function (MTF), and the relative edge response (RER), all of which are key components of image quality, along with signal-to-noise ratio (SNR) and dynamic range. Knowledge of spatial resolution parameters is important to determine if features of interest are distinguishable in imagery or associated products, and to develop image restoration algorithms.

An automated Spatial Resolution Verification Tool (SRVT) was developed to rapidly determine the spatial resolution characteristics of remotely sensed aerial and satellite imagery. Most current methods for assessing spatial resolution characteristics of imagery rely on pre-deployed engineered targets and are performed only at selected times within preselected scenes. The SRVT addresses these insufficiencies by finding uniform, high-contrast edges from urban scenes and then using these edges to determine standard estimators of spatial resolution, such as the MTF and the RER.

The SRVT was developed using the MATLAB® programming language and environment. This automated software algorithm assesses every image in an acquired data set, using edges found within each image, and in many cases eliminating the need for dedicated edge targets. The SRVT automatically identifies high-contrast, uniform edges and calculates the MTF and RER of each image, and when possible, within sections of an image, so that the variation of spatial resolution characteristics across the image can be analyzed. The automated algorithm is capable of quickly verifying the spatial resolution quality of all images within a data set, enabling the appropriate use of those images in a number of applications.

The SRVT has been validated against traditional techniques using IKONOS and QuickBird satellite imagery of NASA Stennis Space Center engineered edge targets. Preliminary comparisons of SRVT-estimated spatial resolution from naturally occurring edges against those obtained using traditional techniques show excellent agreement.

The SRVT can be used to evaluate the image quality of a single image, a product over time, and products from different systems. In addition to the above image quality metrics, the output of the SRVT could be used to estimate National Imagery Interpretability Rating Scale (NIIRS) values for panchromatic imagery, and serve as the basis for developing multispectral image-quality metrics.

This work was done by Bruce Davis of Stennis Space Center, Robert Ryan and Kara Holekamp of Science Systems and Applications, Inc., and Ronald Vaughn of Computer Sciences Corporation. For more information Contact the Office of the Chief Technologist at Stennis Space Center, (228) 688-1929. Refer to SSC-00339.

Electrical Connector Mechanical Seating Sensor

John F. Kennedy Space Center, Florida

A sensor provides a measurement of the degree of seating of an electrical connector. This sensor provides a number of discrete distances that a plug is inserted into a socket or receptacle. The number of measurements is equal to the number of pins available in the connector for sensing.

On at least two occasions, the Shuttle Program has suffered serious time delays and incurred excessive costs simply because a plug was not seated well within a receptacle. Two methods were designed to address this problem: (1) the resistive pin technique and (2) the discrete

length pins technique. In the resistive pin approach, a standard pin in a male connector is replaced with a pin that has a uniform resistivity along its length. This provides a variable resistance on that pin that is dependent on how far the pin is inserted into a socket. This is essentially a linear potentiometer.

The discrete approach uses a pin (or a few pins) in the connector as a displacement indicator by truncating the pin length so it sits shorter in the connector than the other pins. A loss of signal on this pin would indicate a discrete amount of displacement of the connector. This approach would only give discrete values of connector displacement, and at least one pin would be needed for each displacement value that would be of interest.

This work was done by Ellen Arens, Janine Captain, and Robert Youngquist of Kennedy Space Center. Further information is contained in a TSP (see page 1). **KSC-13210/559**

In Situ Aerosol Detector

Goddard Space Flight Center, Greenbelt, Maryland

An affordable technology designed to facilitate extensive global atmospheric aerosol measurements has been developed. This lightweight instrument is compatible with newly developed platforms such as tethered balloons, blimps, kites, and even disposable instruments such as dropsondes. This technology is based on detection of light scattered by aerosol particles where an optical layout is used to enhance the performance of the laboratory prototype instrument, which allows detection of smaller aerosol particles and improves the accuracy of aerosol particle size measurement.

It has been determined that using focused illumination geometry without any apertures is advantageous over using the originally proposed collimated beam/slit geometry (that is supposed to produce uniform illumination over the beam cross-section). The illumination source is used more efficiently, which allows detection of smaller aerosol particles. Second, the obtained integral scattered light intensity measured for the particle can be corrected for the beam intensity profile inhomogeneity based on the measured beam intensity profile and measured particle location. The particle location (coordinates) in the illuminated sample volume is determined based on the information contained in the image frame. The procedure considerably improves the accuracy of determination of the aerosol particle size.

This work was done by Andrei Vakhtin of Vista Photonics and Lev Krasnoperov of New Jersey Institute of Technology for Goddard Space Flight Center. Further information is contained in a TSP (see page 1). **GSC-15879-1**

Multi-Parameter Aerosol Scattering Sensor

John H. Glenn Research Center, Cleveland, Ohio

This work relates to the development of sensors that measure specific aerosol properties. These properties are in the form of integrated moment distributions, i.e., total surface area, total mass, etc., or mathematical combinations of these moment distributions. Specifically, the innovation involves two fundamental features: a computational tool to design and optimize such sensors and the embodiment of these sensors in actual practice.

The measurement of aerosol properties is a problem of general interest. Applications include, but are not limited to, environmental monitoring, assessment of human respiratory health, fire detection, emission characterization and control, and pollutant monitoring. The objectives for sensor development include increased accuracy and/or dynamic range, the inclusion in a single sensor of the ability to measure multiple aerosol properties, and developing an overall physical package that is rugged, compact, and low in power consumption, so as to enable deployment in harsh or confined field applications, and as distributed sensor networks. Existing instruments for this purpose include scattering photometers, direct-reading mass instruments, Beta absorption devices, differential mobility analyzers, and gravitational samplers.

The family of sensors reported here is predicated on the interaction of light and matter; specifically, the scattering of light from distributions of aerosol particles. The particular arrangement of the sensor, e.g. the wavelength(s) of incident radiation, the number and location of optical detectors, etc., can be derived so as to optimize the sensor response to aerosol properties of practical interest. A key feature of the design is the potential embodiment as an extremely compact, integrated microsensor package. This is of fundamental importance, as it enables numerous previously inaccessible applications. The embodiment of these sensors is inherently low maintenance and high reliability by design.

The novel and unique features include the underlying computational underpinning that allows the optimization for specific applications, and the physical embodiment that affords the construction of a compact, durable, and reliable integrated package. The advantage appears in the form of increased accuracy relative to existing instruments, and the applications enabled by the physical attributes of the resulting configuration.

This work was done by Paul S. Greenberg and David G. Fischer of Glenn Research Center. Further information is contained in a TSP (see page 1).

Inquiries concerning rights for the commercial use of this invention should be addressed to NASA Glenn Research Center, Innovative Partnerships Office, Attn: Steven Fedor, Mail Stop 4–8, 21000 Brookpark Road, Cleveland, Ohio 44135. Refer to LEW-18634-1.

MOSFET Switching Circuit Protects Shape Memory Alloy Actuators

John H. Glenn Research Center, Cleveland, Ohio

A small-footprint, full surface-mount-component printed circuit board employs MOSFET (metal-oxide-semiconductor field-effect transistor) power switches to switch high currents from any input power supply from 3 to 30 V.

High-force shape memory alloy (SMA) actuators generally require high current (up to 9 A at 28 V) to actuate. SMA wires (the driving element of the actuators) can be quickly overheated if power is not removed at the end of stroke, which can damage the wires. The new analog driver prevents overheating of the SMA wires in an actuator by momentarily removing power when the end limit switch is closed, thereby allowing complex control schemes to be adopted without concern for overheating. Either an integral pushbutton or microprocessor-controlled gate or control line inputs switch current to the actuator until the end switch line goes from logic high to logic low state. Power is then momentarily removed (switched off by the MOSFET). The analog driver is suited to use with nearly any SMA actuator.

This work was done by Mark A. Gummin of Miga Motor Company for Glenn Research Center. Further information is contained in a TSP (see page 1).

Inquiries concerning rights for the commercial use of this invention should be addressed to NASA Glenn Research Center, Innovative Partnerships Office, Attn: Steven Fedor, Mail Stop 4–8, 21000 Brookpark Road, Cleveland, Ohio 44135. Refer to LEW-18581-1.

Optimized FPGA Implementation of Multi-Rate FIR Filters Through Thread Decomposition

This technique is used in design automation and in digital circuit design.

NASA's Jet Propulsion Laboratory, Pasadena, California

Multi-rate finite impulse response (MRFIR) filters are among the essential signal-processing components in spaceborne instruments where finite impulse response filters are often used to minimize nonlinear group delay and finite-precision effects. Cascaded (multi-stage) designs of MRFIR filters are further used for large rate change ratio in order to lower the required throughput, while simultaneously achieving comparable or better performance than single-stage designs. Traditional representation and implementation of MRFIR employ polyphase decomposition of the original filter structure, whose main purpose is to compute only the needed output at the lowest possible sampling rate.

In this innovation, an alternative representation and implementation technique called TD-MRFIR (Thread Decomposition MRFIR) is presented. The basic idea is to decompose MRFIR into output computational threads, in contrast to a structural decomposition of the original filter as done in the polyphase decomposition. A naïve implementation of a decimation filter consisting of a full FIR followed by a downsampling stage is very inefficient, as most of the computations performed by the FIR state are discarded through downsampling. In fact, only $1/M$ of the total computations are useful (M being the decimation factor). Polyphase decomposition provides an alternative view of decimation filters, where the downsampling occurs before the FIR stage, and the outputs are viewed as the sum of M sub-filters with length of N/M taps. Although this approach leads to more efficient filter designs, in general the implementation is not straightforward if the numbers of multipliers need to be minimized.

In TD-MRFIR, each thread represents an instance of the finite convolution required to produce a single output of the MRFIR. The filter is thus viewed as a finite collection of concurrent threads. Each of the threads completes when a convolution result (filter output value) is computed, and activated when the first input of the convolution becomes available. Thus, the new threads get spawned at exactly the rate of N/M, where N is the total number of taps, and M is the decimation factor. Existing threads retire at the same rate of N/M. The implementation of an MRFIR is thus transformed into a problem to statically schedule the minimum number of multipliers such that all threads can be completed on time. Solving the static scheduling problem is rather straightforward if one examines the Thread Decomposition Diagram, which is a table-like diagram that has rows representing computation threads and columns representing time. The control logic of the MRFIR can be implemented using simple counters. Instead of decomposing MRFIRs into sub-filters as suggested by polyphase decomposition, the thread decomposition diagrams transform the problem into a familiar one of static scheduling, which can be easily solved as the input rate is constant.

This work was done by Kayla N. Kobayashi, Yutao He, and Jason X. Zheng of Caltech for NASA's Jet Propulsion Laboratory. For more information, contact iaoffice@jpl.nasa.gov. NPO-47409

Circuit for Communication Over Power Lines

This technique can be used in vehicle sensors, building sensors, and other industrial control applications.

John H. Glenn Research Center, Cleveland, Ohio

Many distributed systems share common sensors and instruments along with a common power line supplying current to the system. A communication technique and circuit has been developed that allows for the simple inclusion of an instrument, sensor, or actuator node within any system containing a common power bus. Wherever power is available, a node can be added, which can then draw power for itself, its associated sensors, and actuators from the power bus all while communicating with other nodes on the power bus.

The technique modulates a DC power bus through capacitive coupling using on-off keying (OOK), and receives and demodulates the signal from the DC power bus through the same capacitive coupling. The circuit acts as serial modem for the physical power line communication. The circuit and technique can be made of commercially available components or included in an application specific integrated circuit (ASIC) design, which allows for the circuit to be included in current designs with additional circuitry or embedded into new designs.

This device and technique moves computational, sensing, and actuation abilities closer to the source, and allows for the networking of multiple similar nodes to each other and to a central processor. This technique also allows for reconfigurable systems by adding or removing nodes at any time. It can do so using nothing more than the *in situ* power wiring of the system.

This work was done by Michael J. Krasowski, Normal F. Prokop, Lawrence C. Greer III, and Jennifer Nappier of Glenn Research Center. Further information is contained in a TSP (see page 1).

Inquiries concerning rights for the commercial use of this invention should be addressed to NASA Glenn Research Center, Innovative Partnerships Office, Attn: Steven Fedor, Mail Stop 4–8, 21000 Brookpark Road, Cleveland, Ohio 44135. Refer to LEW-18631-1.

High-Efficiency Ka-Band Waveguide Two-Way Asymmetric Power Combiner

This device is applicable for use with high-power MMIC solid-state amplifiers.

John H. Glenn Research Center, Cleveland, Ohio

NASA is planning a number of Space Exploration, Earth Observation and Space Science missions where Ka-band solid-state power amplifiers (SSPAs) could have a role. Monolithic microwave integrated circuit (MMIC) based SSPAs with output powers on the order of 10 W at Ka-band frequencies would be adequate to satisfy the data transmission rate requirements at the distances involved. MMICs are a type of integrated circuit fabricated on a GaAs wafer, which operates at microwave frequencies and performs the function of signal amplification. The highest power Ka-band (31.8 to 32.3 GHz) SSPA to have flown in space had an output power of 2.6 W with an overall efficiency of 14.3 percent. This SSPA was built around discrete GaAs pHEMT (high electron mobility transistor) devices and flew aboard the Deep Space One spacecraft. State-of-the-art GaAs pHEMT-based MMIC power amplifiers (PAs) can deliver RF power at Ka-band frequencies anywhere from 3 W with a power added efficiency (PAE) of 32 percent to 6 W with a PAE of 26 percent. However, to achieve power levels higher than 6 W, the output of several MMIC PAs would need to be combined using a high-efficiency power combiner. Conventional binary waveguide power combiners, based on short-slot and magic-T circuits, require MMIC PAs with identical amplitude and phase characteristics for high combining efficiency. However, due to manufacturing process variations, the output powers of the MMIC PAs tend to be unequal, and hence the need to develop unequal power combiners.

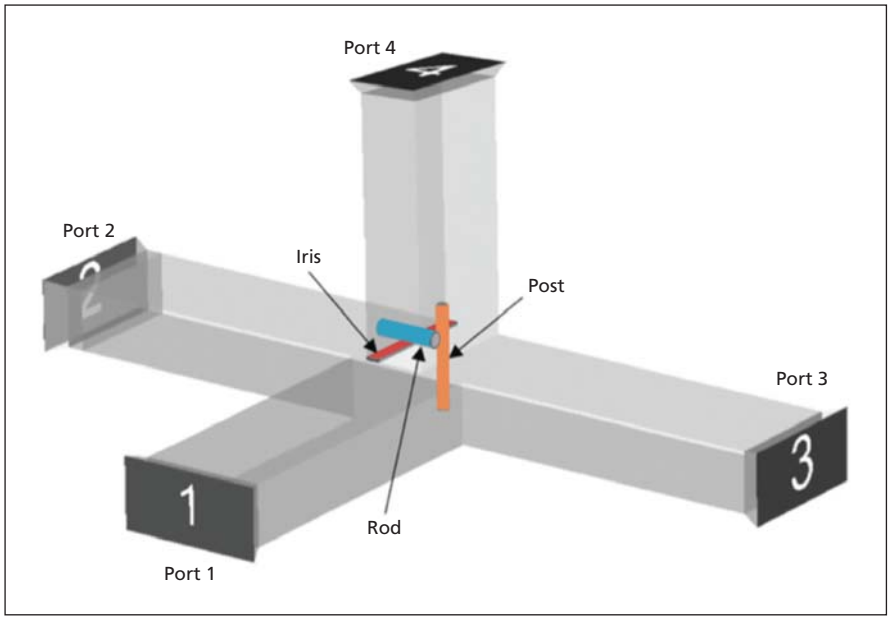

Transparent view of **Asymmetric Combiner** showing port configuration and relative orientation of rod, post, and iris.

A two-way asymmetric magic-T based power combiner for MMIC power amplifiers, which can take in unequal inputs, has been successfully designed, fabricated, and characterized over NASA's Deep Space Network (DSN) frequency range of 31.8 to 32.3 GHz. The figure is a transparent view of the asymmetric combiner that shows the 4-port configuration and the internal structure. The rod, post, and iris are positioned by design to achieve the desired asymmetric power ratio, phase equality, and port isolation. Although the combiner was designed for an input power ratio of 2:1, it can be custom-designed for any arbitrary power ratio and frequency range. The manufactured prototype combiner was precision machined from aluminum and is less than 2 in.^{3} (32.8 cm^3). Previously investigated rectangular waveguide unequal power combiners were based on shunt/series coupling slots, E-plane septums, or H-plane T-junctions. All the prior art unequal power combiners operated at or below X-band (10 GHz) frequencies and were primarily used in the feed network of antenna arrays. The only reported asymmetric magic-T was developed as a 2:1 power divider for operation at a much lower frequency, around 500 MHz.

The measured power ratio when tested as a power divider was very close to 2 and the phase balance was within 2.6°, resulting in near ideal performance. When tested as a combiner using two MMIC SSPAs with a 2:1 power output ratio, an efficiency greater than 90 percent was demonstrated over the 500 MHz DSN frequency range. The return loss at the combiner output port (1) was greater than 18 dB and the input port (2 and 3) isolation was greater than 22 dB. The results show the asymmetric combiner to be a good candidate for high-efficiency power combining of two or more SSPAs needed to achieve the 6 to 10 W required by space communications systems of future NASA missions.

This work was done by E.G. Wintucky, R.N. Simons, and J.C. Freeman of Glenn Research Center and C.T. Chevalier of QinetiQ North America Corp. Further information is contained in a TSP (see page 1).

Inquiries concerning rights for the commercial use of this invention should be addressed to NASA Glenn Research Center, Innovative Partnerships Office, Attn: Steven Fedor, Mail Stop 4–8, 21000 Brookpark Road, Cleveland, Ohio 44135. Refer to LEW-18590-1.

10–100 Gbps Offload NIC for WAN, NLR, and Grid Computing

Goddard Space Flight Center, Greenbelt, Maryland

An extremely fast offload engine system has been developed that operates at 60 Gigabits per second (Gbps), and has scalability to 100 Gbps full-duplex (f-d). This system is based on unique coding and architecture derived from splintered UDP (User Datagram Protocol) offload technology, resulting in unique FPGA (field programmable gate array) intellectual property core and firmware.

This innovation improves the networking speed of supercomputer clusters by providing an ultra-fast network protocol processing offload from a CPU (central processing unit) by inserting an offload engine into a host backplane and network connections. This runs on protocol firmware.

This work was done by Patricia Crowley of Gonzaga University, James Awrach of SeaFire, and Arthur Maccabe of the University of New Mexico for Goddard Space Flight Center. Further information is contained in a TSP (see page 1). *GSC-15447-1*

Pulsed Laser System to Simulate Effects of Cosmic Rays in Semiconductor Devices

The system can measure the radiation sensitivity of microelectronic devices with high spatial and temporal resolution.

NASA's Jet Propulsion Laboratory, Pasadena, California

Spaceflight system electronic devices must survive a wide range of radiation environments with various particle types including energetic protons, electrons, gamma rays, x-rays, and heavy ions. High-energy charged particles such as heavy ions can pass straight through a semiconductor material and interact with a charge-sensitive region, generating a significant amount of charge (electron-hole pairs) along their tracks. These excess charges can damage the device, and the response can range from temporary perturbations to permanent changes in the state or performance. These phenomena are called single event effects (SEE).

Before application in flight systems, electronic parts need to be qualified and tested for performance and radiation sensitivity. Typically, their susceptibility to SEE is tested by exposure to an ion beam from a particle accelerator. At such facilities, the device under test (DUT) is irradiated with large beams so there is no fine resolution to investigate particular regions of sensitivity on the parts. While it is the most reliable approach for radiation qualification, these evaluations are time consuming and costly. There is always a need for new cost-efficient strategies to complement accelerator testing: pulsed lasers provide such a solution.

Pulsed laser light can be utilized to simulate heavy ion effects with the advantage of being able to localize the sensitive region of an integrated circuit. Generally, a focused laser beam of approximately picosecond pulse duration is used to generate carrier density in the semiconductor device. During irradiation, the laser pulse is absorbed by the electronic medium with a wavelength selected accordingly by the user, and the laser energy can ionize and simulate SEE as would occur in

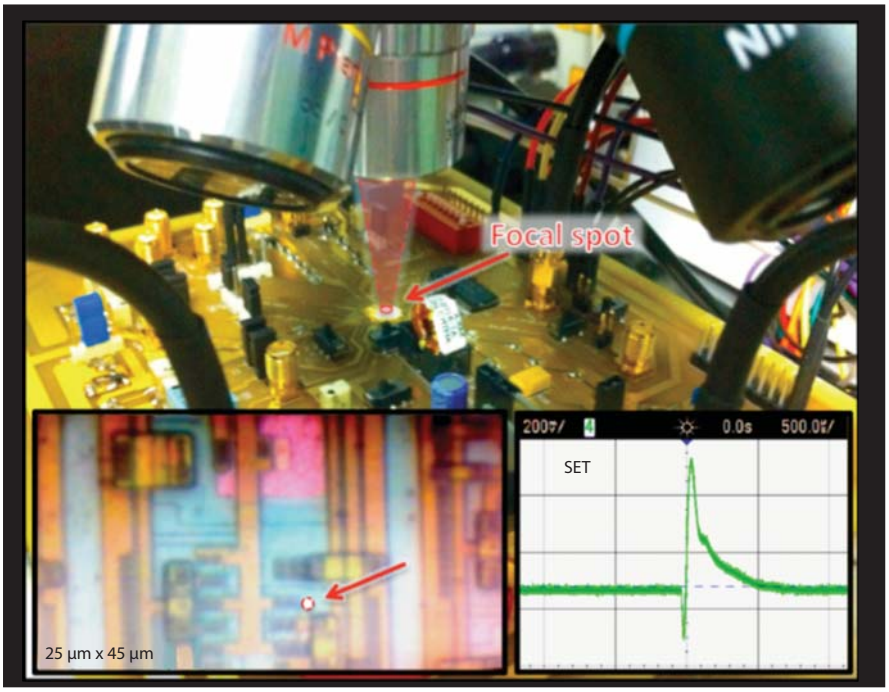

This figure illustrates the ps-pulsed **Laser Beam Path** focused to a micron spot onto a semiconductor device. The lower left inset shows the magnified image through the microscope indicating the laser's focal spot. In the lower right inset, a single event transient (SET) was captured by the digital scope due to a single pulse of 20 nJ. The peak amplitude is ≈400 mV with ≈200-µs decay.

space. With a tightly focused near infrared (NIR) laser beam, the beam waist of about a micrometer can be achieved, and additional scanning techniques are able to yield submicron resolution. This feature allows mapping of all of the sensitive regions of the studied device with fine resolution, unlike heavy ion experiments. The problematic regions can be precisely identified, and it provides a considerable amount of information about the circuit. In addition, the system allows flexibility for testing the device in different configurations *in situ*.

JPL has built and tested a pulsed laser facility with a mode-locked Ti:sapphire cavity pumped by a 5-W diode-pumped solid-state laser at 532 nm. A laser beam with a pulse width of about 2 picoseconds is tightly focused through a microscope objective onto the DUT. The Ti:sapphire has a wavelength range of 720–850 nm, with average power ranging from about 500 mW to as high as 1 W at 780 nm. The cavity outputs an 80-MHz repetition rate of pulses, which are precisely selected by an acoustic-optical modulator (AOM). The beam power can be attenuated to deliver calibrated energy to the DUT, typically chosen in the range of 1 to 500 pJ. When focused to a micron-scale waist, the electromagnetic radiation intensity ionizes the silicon medium to a penetration depth determined by the wavelength, and induces SEE within the device medium, simulating a heavy ion penetrating into the part.

The laser system utilizes the tunable pulsed source along with a HeNe laser continuous wave source at 635 nm for alignment guidance. It also incorporates a motorized two-axis stage to move the DUT and scan the area with resolution down to 100 nm. With automated computer control of the pulses, stage, and digital oscilloscope, the system can record the voltage transient responses as it steps through a pre-set scanning area, thereby generating a functional map of the device sensitivity with extremely fine resolution.

While it cannot fully replace heavy ion testing, this pulsed laser technology is a necessary complementary tool that helps the radiation hardness assurance flow when qualifying electronics for space applications. It also offers high-resolution imaging of the device sensitivity to localize problematic areas of the integrated circuits under test. This spatial and temporal information allows parts to be analyzed and issues to be diagnosed for research and development, leading to more robust and better-performing electronics for space applications.

This work was done by David C. Aveline, Philippe C. Adell, Gregory R. Allen, Steven M. Guertin, and Steven S. McClure of Caltech for NASA's Jet Propulsion Laboratory. Further information is contained in a TSP (see page 1). ***NPO-47254***

Software

Flight Planning in the Cloud

This new interface will enable Principal Investigators (PIs), as well as UAVSAR (Uninhabited Aerial Vehicle Synthetic Aperture Radar) members to do their own flight planning and time estimation without having to request flight lines through the science coordinator. It uses an all-in-one Google Maps interface, a JPL hosted database, and PI flight requirements to design an airborne flight plan. The application will enable users to see their own flight plan being constructed interactively through a map interface, and then the flight planning software will generate all the files necessary for the flight. Afterward, the UAVSAR team can then complete the flight request, including calendaring and supplying requisite flight request files in the expected format for processing by NASA's airborne science program.

Some of the main features of the interface include drawing flight lines on the map, nudging them, adding them to the current flight plan, and reordering them. The user can also search and select takeoff, landing, and intermediate airports. As the flight plan is constructed, all of its components are constantly being saved to the database, and the estimated flight times are updated. Another feature is the ability to import flight lines from previously saved flight plans.

One of the main motivations was to make this Web application as simple and intuitive as possible, while also being dynamic and robust. This Web application can easily be extended to support other airborne instruments.

This work was done by Sarah L. Flores, Bruce D. Chapman, Wayne W. Tung, and Yang Zheng of Caltech for NASA's Jet Propulsion Laboratory. For more information, contact iaoffice@jpl.nasa.gov.

This software is available for commercial licensing. Please contact Daniel Broderick of the California Institute of Technology at danielb@caltech.edu. Refer to NPO-47472.

MPS Editor

Previously, it was time-consuming to hand-edit data and then set up simulation runs to find the effect and impact of the input data on a spacecraft. MPS Editor provides the user the capability to create/edit/update models and sequences, and immediately try them out using what appears to the user as one piece of software. MPS Editor provides an integrated sequencing environment for users. It provides them with software that can be utilized during development as well as actual operations. In addition, it provides them with a single, consistent, user friendly interface.

MPS Editor uses the Eclipse Rich Client Platform to provide an environment that can be tailored to specific missions. It provides the capability to create and edit, and includes an Activity Dictionary to build the simulation spacecraft models, build and edit sequences of commands, and model the effects of those commands on the spacecraft.

MPS Editor is written in Java using the Eclipse Rich Client Platform. It is currently built with four perspectives: the Activity Dictionary Perspective, the Project Adaptation Perspective, the Sequence Building Perspective, and the Sequence Modeling Perspective. Each perspective performs a given task. If a mission doesn't require that task, the unneeded perspective is not added to that project's delivery.

In the Activity Dictionary Perspective, the user builds the project-specific activities, observations, calibrations, etc. Typically, this is used during the development phases of the mission, although it can be used later to make changes and updates to the Project Activity Dictionary. In the Adaptation Perspective, the user creates the spacecraft models such as power, data store, etc. Again, this is typically used during development, but will be used to update or add models of the spacecraft. The Sequence Building Perspective allows the user to create a sequence of activities or commands that go to the spacecraft. It provides a simulation of the activities and commands that have been created.

This work was done by William S. Mathews, Ning Liu, Laurie K. Francis, Taifun L. O'Reilly, Mitchell Schrock, Dennis N. Page, John R. Morris, Joseph C. Joswig, Thomas M. Crockett, and Khawaja S. Shams of Caltech for NASA's Jet Propulsion Laboratory. For more information, contact iaoffice@jpl.nasa.gov.

This software is available for commercial licensing. Please contact Daniel Broderick of the California Institute of Technology at danielb@caltech.edu. Refer to NPO-47237.

Object-Oriented Multidisciplinary Design, Analysis, and Optimization Tool

An Object-Oriented Optimization (O^3) tool was developed that leverages existing tools and practices, and allows the easy integration and adoption of new state-of-the-art software. At the heart of the O^3 tool is the Central Executive Module (CEM), which can integrate disparate software packages in a cross platform network environment so as to quickly perform optimization and design tasks in a cohesive, streamlined manner. This object-oriented framework can integrate the analysis codes for multiple disciplines instead of relying on one code to perform the analysis for all disciplines.

The CEM was written in FORTRAN and the script commands for each performance index were submitted through the use of the FORTRAN "Call System" command. In this CEM, the user chooses an optimization methodology, defines objective and constraint functions from performance indices, and provides starting and side constraints for continuous as well as discrete design variables.

The structural analysis modules such as computations of the structural weight, stress, deflection, buckling, and flutter and divergence speeds have been developed and incorporated into the O^3 tool to build an object-oriented Multidisciplinary Design, Analysis, and Optimization (MDAO) tool.

This work was done by Chan-gi Pak of Dryden Flight Research Center. Further information is contained in a TSP (see page 1).
DRC-010-013

Cryogenic-Compatible Winchester Connector Mount and Retaining System for Composite Tubes

Goddard Space Flight Center, Greenbelt, Maryland

A connector retainer and mounting system has been designed to replace screw-mounting of Winchester connectors. Countersunk screws are normally used to secure connectors to structures, and to keep them from coming apart. These screws are normally put into threaded or through-holes in metallic structures. This unique retainer is designed such that integral posts keep the connector halves retained, and a groove permits a cable tie to be fastened around the retainer and composite tube, thus securing the connector to the structure.

The system is compatible for use on cryogenic (and conventional) bonded composite tube assemblies. Screws and tapped/through-holes needed to retain and mount Winchester connectors cannot be used on blind-access composite tubes. This system allows for rapid installation, removal, low-molecular-outgassing materials, and particulate-free installation and removal. Installation and/or changes late in the integration, and test flow with limited access in a cleanroom environment are possible. No sanding or bonding is needed.

This work was done by James Pontius and Douglas McGuffey of Goddard Space Flight Center. Further information is contained in a TSP (see page 1). *GSC-16028-1*

Development of Position-Sensitive Magnetic Calorimeters for X-Ray Astronomy

These calorimeters can be used in x-ray metrology, materials microanalysis, and medical applications.

Goddard Space Flight Center, Greenbelt, Maryland

Metallic magnetic calorimeters (MMC) are one of the most promising devices to provide very high energy resolution needed for future astronomical x-ray spectroscopy. MMC detectors can be built to large detector arrays having thousands of pixels. Position-sensitive magnetic (PoSM) microcalorimeters consist of multiple absorbers thermally coupled to one magnetic microcalorimeter. Each absorber element has a different thermal coupling to the MMC, resulting in a distribution of different pulse shapes and enabling position discrimination between the absorber elements. PoSMs therefore achieve the large focal plane area with fewer number of readout channels without compromising spatial sampling.

Excellent performance of PoSMs was achieved by optimizing the designs of key parameters such as the thermal conductance among the absorbers, magnetic sensor, and heat sink, as well as the absorber heat capacities. Microfabrication techniques were developed to construct four-absorber PoSMs, in which each absorber consists of a two-layer composite of bismuth and gold. The energy resolution (FWHM — full width at half maximum) was measured to be better than 5 eV at 6 keV x-rays for all four absorbers. Position determination was demonstrated with pulse-shape discrimination, as well as with pulse rise time.

X-ray microcalorimeters are usually designed to thermalize as quickly as possible to avoid degradation in energy resolution from position dependence to the pulse shapes. Each pixel consists of an absorber and a temperature sensor, both decoupled from the cold bath through a weak thermal link. Each pixel requires a separate readout channel; for instance, with a SQUID (superconducting quantum interference device). For future astronomy missions where thousands to millions of resolution elements are required, having an individual SQUID readout channel for each pixel becomes difficult. One route to attaining these goals is a position-sensitive detector in which a large continuous or pixilated array of x-ray absorbers shares fewer numbers of temperature sensors.

A means of discriminating the signals from different absorber positions, however, needs to be built into the device for each sensor. The design concept for the device is such that the shape of the temperature pulse with time depends on the location of the absorber. This inherent position sensitivity of the signal is then analyzed to determine the location of the event precisely, effectively yielding one device with many sub-pixels. With such devices, the total number of electronic channels required to read out a given number of pixels is significantly reduced.

PoSMs were developed that consist of four discrete absorbers connected to a single magnetic sensor. The design concept can be extended to more than four absorbers per sensor. The thermal conductance between the sensor and each absorber is different by design and consequently, the pulse shapes are different depending upon which absorber the x-rays are received, allowing position discrimination. A magnetic sensor was used in which a paramagnetic Au:Er temperature-sensitive material is located in a weak magnetic field.

Deposition of energy from an x-ray photon causes an increase in temperature, which leads to a change of magnetization of the paramagnetic sensor, which is subsequently read out using a low noise dc-SQUID. The PoSM microcalorimeters are fully microfabricated: the Au:Er sensor is located above the meander, with a thin insula-

tion gap in between. For this position-sensitive device, four electroplated absorbers are thermally linked to the sensor via heat links of different thermal conductance. One pixel is identical to that of a single-pixel design, consisting of an overhanging absorber fabricated directly on top of the sensor. It is therefore very strongly thermally coupled to it. The three other absorbers are supported directly on a silicon-nitride membrane. These absorbers are thermally coupled to the sensor via Ti (5 nm)/Au (250 nm) metal links. The strength of the links is parameterized by the number of gold squares making up the link.

For detector performance, experimentally different pulse-shapes were demonstrated with 6 keV x-rays, which clearly show different rise times for different absorber positions. For energy resolution measurement, the PoSM was operated at 32 mK with an applied field that was generated using a persistent current of 50 mA. Over the four pixels, energy resolution ranges from 4.4 to 4.7 eV were demonstrated.

This work was done by Simon Bandler, Thomas Stevenson, and Wen-Ting Hsieh of Goddard Space Flight Center. Further information is contained in a TSP (see page 1).
GSC-15907-1

Planar Rotary Piezoelectric Motor Using Ultrasonic Horns

These motors are scalable and can be used in small systems such as motors in electronic cameras or small flight instruments.

NASA's Jet Propulsion Laboratory, Pasadena, California

A motor involves a simple design that can be embedded into a plate structure by incorporating ultrasonic horn actuators into the plate. The piezoelectric material that is integrated into the horns is pre-stressed with flexures. Piezoelectric actuators are attractive for their ability to generate precision high strokes, torques, and forces while operating under relatively harsh conditions (temperatures at single-digit K to as high as 1,273 K).

Electromagnetic motors (EM) typically have high rotational speed and low torque. In order to produce a useful torque, these motors are geared down to reduce the speed and increase the torque. This gearing adds mass and reduces the efficiency of the EM. Piezoelectric motors can be designed with high torques and lower speeds directly without the need for gears.

Designs were developed for producing rotary motion based on the Barth concept of an ultrasonic horn driving a rotor. This idea was extended to a linear motor design by having the horns drive a slider. The unique feature of these motors is that they can be designed in a monolithic planar structure. The design is a unidirectional motor, which is driven by eight horn actuators, that rotates in the clockwise direction. There are two sets of flexures. The flexures around the piezoelectric material are pre-stress flexures and they pre-load the piezoelectric disks to maintain their being operated under compression when electric field is applied. The other set of flexures is a mounting flexure that attaches to the horn at the nodal point and can be designed to generate a normal force between the horn tip and the rotor so that to first order it operates independently and compensates for the wear between the horn and the rotor.

This motor could be stacked to increase the torque on the rotor, or flipped and stacked to produce bidirectional rotation. The novel features of this motor are:

- A monolithic planar piezoelectric motor driven by high-power ultrasonic horns that can be manufactured from a single piece of metal using EDM (electric discharge machining), precision machining, or rapid prototyping.
- A plate structure that can rotate a rotor in a plane.
- A flexure system with low stiffness that accommodates mechanical wear at the rotor horn interface and maintains a constant normal force.
- The ability to embed many horns in a plate to increase the torque.
- A rotary actuator that can be designed to rotate clockwise or counterclockwise, depending on the direction of extension of the horn with respect to the center axis of the rotor.
- A linear actuation mechanism that operates bidirectionally in the plate.
- A mechanism that is operated with soft flexure springs that maintains constant normal and hence friction forces in a motor.
- A planar rotary piezoelectric motor that is driven by ultrasonic horns that can be stacked to produce higher torques.
- Actuator plates that can be flipped and stacked to produce bidirectional drive.

This work was done by Stewart Sherrit, Xiaoqi Bao, Mircea Badescu, and Yoseph Bar-Cohen of Caltech; Daniel Geiyer of Rochester Institute of Technology; and Patrick N. Ostlund and Phillip Allen of Cal Poly Pomona for NASA's Jet Propulsion Laboratory. Further information is contained in a TSP (see page 1). *NPO-47813*

Self-Rupturing Hermetic Valve

NASA's Jet Propulsion Laboratory, Pasadena, California

For commercial, military, and aerospace applications, low-cost, small, reliable, and lightweight gas and liquid hermetically sealed valves with post initiation on/off capability are highly desirable for pressurized systems. Applications include remote fire suppression, single-use system-pressurization systems, spacecraft propellant systems, and *in situ* instruments. Current pyrotechnic-activated rupture disk hermetic valves were designed for physically larger systems and are heavy and integrate poorly with portable equipment, aircraft, and small spacecraft and instrument systems. Additionally, current pyrotechnically activated systems impart high g-force shock loads to surrounding components and structures, which increase the risk of damage and can require additional mitigation.

The disclosed mechanism addresses the need for producing a hermetically sealed micro-isolation valve for low and high pressure for commercial, aerospace, and spacecraft applications. High-precision electrical discharge machining (EDM) parts allow for the machining of mated parts with gaps less than a thousandth of an inch. These high-precision parts are used to support against pressure and extrusion, a thin hermetically welded diaphragm. This diaphragm ruptures from a pressure differential when the support is removed and/or when the plunger is forced against the diaphragm. With the addition of conventional seals to the plunger and a two-way actuator, a derivative of this design would allow non-hermetic use as an on/off or metering valve after the initial rupturing of the hermetic sealing disk. In addition, in a single-use hermetically sealed isolation valve, the valve can be activated without

the use of potential leak-inducing valve body penetrations.

One implementation of this technology is a high-pressure, high-flow-rate rupture valve that is self-rupturing, which is advantageous for high-pressure applications such as gas isolation valves. Once initiated, this technology is self-energizing and requires low force compared to current pyrotechnic-based burst disk hermetic valves.

This is a novel design for producing a single-use, self-rupturing, hermetically sealed valve for isolation of pressurized gas and/or liquids. This design can also be applied for single-use disposable valves for chemical instruments. A welded foil diaphragm is fully supported by two mated surfaces that are machined to micron accuracies using EDM. To open the valve, one of the surfaces is moved relative to the other to (a) remove the support creating an unsupported diaphragm that ruptures due to over pressure, and/or (b) produce tension in the diaphragm and rupture it.

This work was done by Curtis E. Tucker Jr. and Stewart Sherrit of Caltech for NASA's Jet Propulsion Laboratory. ***F****Further information is contained in a TSP (see page 1).* *NPO-47497*

Explosive Bolt Dual-Initiated From One Side

Lyndon B. Johnson Space Center, Houston, Texas

An explosive bolt has been developed that has a one-sided dual initiation train all the way down to the pyro charge for high reliability, while still allowing the other side of the bolt to remain in place after actuation to act as a thermal seal in an extremely high-temperature environment. This lightweight separation device separates at a single fracture plane, and has as much redundancy/reliability as possible. The initiation train comes into the explosive bolt from one side.

This work was done by Eric Snow of Lockheed Martin for Johnson Space Center. For further information, contact the JSC Innovation Partnerships Office at (281) 483-3809. MSC-24843-1

Two-Stage Winch for Kites and Tethered Balloons or Blimps

Goddard Space Flight Center, Greenbelt, Maryland

A winch system provides a method for launch and recovery capabilities for kites and tethered blimps or balloons. Low power consumption is a key objective, as well as low weight for portability. This is accomplished by decoupling the tether-line storage and winding/unwinding functions, and providing tailored and efficient mechanisms for each. The components of this system include rotational power input devices such as electric motors or other apparatus, line winding/unwinding reel(s), line storage reel(s), and independent drive trains.

Power is applied to the wind/unwind reels to transport the tether line. Power is also applied to a line storage reel, from either the wind/unwind power source, the wind/unwind reel itself, or separate power source. The speeds of the two reels are synchronized, but not dependent on each other. This is accomplished via clutch mechanisms, variable transmissions, or independent motor controls. The speed of the storage reel is modulated as the effective diameter of the reel changes with line accumulation.

This work was done by Ted Miles and Geoff Bland of Goddard Space Flight Center. Further information is contained in a TSP (see page 1). *GSC-16014-1*

Dampers for Stationary Labyrinth Seals

Spring and/or shot dampers are incorporated as integral parts of seals.

Marshall Space Flight Center, Alabama

Vibration dampers have been invented that are incorporated as components within the stationary labyrinth seal assembly. These dampers are intended to supplement other vibration-suppressing features of labyrinth seals in order to reduce the incidence of high-cycle-fatigue failures, which have been known to occur in the severe vibratory environments of jet engines and turbopumps in which labyrinth seals are typically used. A vibration damper of this type includes several leaf springs and/or a number of metallic particles (shot) all held in an annular seal cavity by a retaining ring. The leaf springs are made of a spring steel alloy chosen, in conjunction with design parameters, to maintain sufficient preload to ensure effectiveness of damping at desired operating temperatures. The cavity is vented via a small radial gap between the retaining ring and seal housing. The damping mechanism is complex. In the case of leaf springs, the mechanism is mainly friction in the slippage between the seal housing and individual dampers. In the case of a damper that contains shot, the damping mechanism includes contributions from friction between individual particles, friction between particles and cavity walls, and dissipation of kinetic energy of impact.

The basic concept of particle/shot vibration dampers has been published previously; what is new here is the use of

such dampers to suppress traveling-wave vibrations in labyrinth seals. Damping effectiveness depends on many parameters, including, but not limited to, coefficient of friction, mode shape, and frequency and amplitude of vibrational modes. In tests, preloads of the order of 6 to 15 lb (2.72 to 6.8 kg) per spring damper were demonstrated to provide adequate damping levels. Effectiveness of shot damping of vibrations having amplitudes from 20 to 200 times normal terrestrial gravitational acceleration (196 to 1,960 m/s^2) and frequencies up to 12 kHz was demonstrated for shot sizes from 0.032 to 0.062 in. (0.8 to 1.6 mm) at fill levels of from 70 to 95 percent.

This work was done by Yehia El-Aini, William Mitchell, Lawrence Roberts, Stuart Montgomery, and Gary Davis of Pratt & Whitney Rocketdyne for Marshall Space Flight Center. For more information, contact Sammy Nabors, MSFC Commercialization Assistance Lead, at sammy.a.nabors@nasa.gov.

Title to this invention has been waived under the provisions of the National Aeronautics and Space Act {42 U.S.C. 2457(f)} to Pratt & Whitney Rocketdyne. Inquiries concerning licenses for its commercial development should be addressed to

Pratt & Whitney Rocketdyne
P.O. Box 109600
West Palm Beach, FL 33410

Refer to MFS-32571-1, volume and number of this NASA Tech Briefs *issue, and the page number.*

Two-Arm Flexible Thermal Strap

This design allows for large elastic displacements in two planes and moderate elasticity in the third plane.

NASA's Jet Propulsion Laboratory, Pasadena, California

Airborne and space infrared cameras require highly flexible direct cooling of mechanically-sensitive focal planes. A thermal electric cooler is often used together with a thermal strap as a means to transport the thermal energy removed from the infrared detector. While effective, traditional thermal straps are only truly flexible in one direction. In this scenario, a cooling solution must be highly conductive, lightweight, able to operate within a vacuum, and highly flexible in all axes to accommodate adjustment of the focal plane while transmitting minimal force.

A two-armed thermal strap using three end pieces and a twisted section offers enhanced elastic movement, significantly beyond the motion permitted by existing thermal straps. This design innovation allows for large elastic displacements in two planes and moderate elasticity in the third plane. By contrast, a more conventional strap of the same conductance offers less flexibility and asymmetrical elasticity.

The two-arm configuration reduces the bending moment of inertia for a given conductance by creating the same cross-sectional area for thermal conduction, but with only half the thickness. This reduction in the thickness has a significant effect on the flexibility since there is a cubic relationship between the thickness and the rigidity or bending moment of inertia.

The novelty of the technology lies in the mechanical design and manufacturing of the thermal strap. The enhanced flexibility will facilitate cooling of mechanically sensitive components (example: optical focal planes).

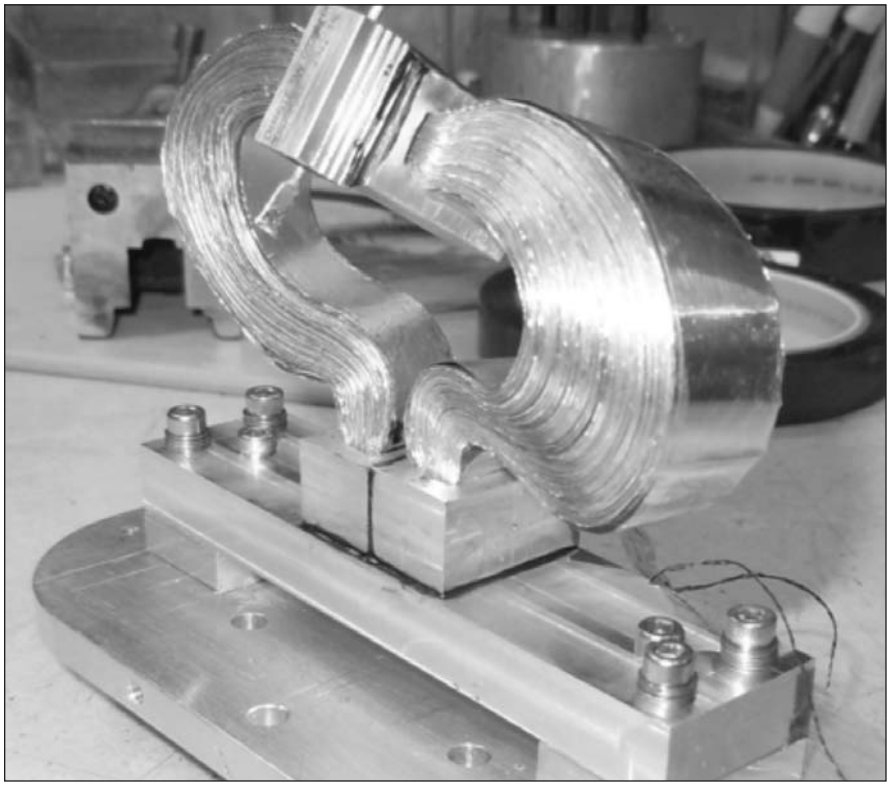

Two-Arm Flexible Thermal Strap

This development is a significant contribution to the thermal cooling of optics. It is known to be especially important in the thermal control of optical focal planes due to their highly sensitive alignment requirements and mechanical sensitivity; however, many other applications exist including the cooling of gimbal-mounted components.

This work was done by Eugenio Urquiza, Cristal Vasquez, Jose I. Rodriguez, Robert S. Leland, and Byron E. Van Gorp of NASA's Jet Propulsion Laboratory. For more information, contact iaoffice@jpl.nasa.gov. NPO-47744

Carbon Dioxide Removal via Passive Thermal Approaches

Lyndon B. Johnson Space Center, Houston, Texas

A paper describes a regenerable approach to separate carbon dioxide from other cabin gases by means of cooling until the carbon dioxide forms carbon dioxide ice on the walls of the physical device. Currently, NASA space vehicles remove carbon dioxide by reaction with lithium hydroxide (LiOH) or by adsorption to an amine, a zeolite, or other sorbent. Use of lithium hydroxide, though reliable and well-understood, requires significant mass for all but the shortest missions in the form of lithium hydroxide pellets, because the reaction of carbon dioxide with lithium hydroxide is essentially irreversible. This approach is regenerable, uses less power than other historical approaches, and it is almost entirely passive, so it is more economical to operate and potentially maintenance-free for long-duration missions.

In carbon dioxide removal mode, this approach passes a "bone-dry" stream of crew cabin atmospheric gas through a metal channel in thermal contact with a radiator. The radiator is pointed to reject thermal loads only to space. Within the channel, the working stream is cooled to the sublimation temperature of carbon dioxide at the prevailing cabin pressure, leading to formation of carbon dioxide ice on the channel walls. After a prescribed time or accumulation of carbon dioxide ice, for regeneration of the device, the channel is closed off from the crew cabin and the carbon dioxide ice is sublimed and either vented to the environment or accumulated for recovery of oxygen in a fully regenerative life support system.

This work was done by Michael Lawson, Anthony Hanford, Bruce Conger, and Molly Anderson of Johnson Space Center. Further information is contained in a TSP (see page 1). *MSC-24445-1*

Polymer Electrolyte-Based Ambient Temperature Oxygen Microsensors for Environmental Monitoring

This oxygen microsensor has extremely low power consumption, is small in size, and is simple to batch-fabricate.

John H. Glenn Research Center, Cleveland, Ohio

An ambient temperature oxygen microsensor, based on a Nafion polymer electrolyte, has been developed and was microfabricated using thin-film technologies. A challenge in the operation of Nafion-based sensor systems is that the conductivity of Nafion film depends on the humidity in the film. Nafion film loses conductivity when the moisture content in the film is too low, which can affect sensor operation. The advancement here is the identification of a method to retain the operation of the Nafion films in lower humidity environments. Certain salts can hold water molecules in the Nafion film structure at room temperature. By mixing salts with the Nafion solution, water molecules can be homogeneously distributed in the Nafion film increasing the film's hydration to prevent Nafion film from being dried out in low-humidity environment. The presence of organics provides extra sites in the Nafion film to promote proton (H^+) mobility and thus improving Nafion film conductivity and sensor performance.

The fabrication of ambient temperature oxygen microsensors includes depositing basic electrodes using noble metals, and metal oxides layer on one of the electrode as a reference electrode. The use of noble metals for electrodes is due to their strong catalytic properties for oxygen reduction. A conducting polymer Nafion, doped with water-retaining components and extra sites facilitating proton movement, was used as the electrolyte material, making the design adequate for low humidity environment applications. The Nafion solution was coated on the electrodes and air-dried. The sensor operates at room temperature in potentiometric mode, which measures voltage differences between working and reference electrodes in different gases. Repeatable responses to 21-percent oxygen in nitrogen were achieved using nitrogen as a baseline gas. Detection of oxygen from 7 to 21 percent has also been demonstrated.

The room-temperature oxygen microsensor developed has extremely low power consumption (no heating for operation, no voltage applied to the sensor, only a voltmeter is needed to measure the output), is small in size, is simple to batch-fabricate, and is high in sensor yield. It is applicable in a wide humidity range, with improved operation in low humidity after the additives were added to the Nafion film. Through further improvement and development, the sensor can be used for aerospace applications such as fuel leak detection, fire detection, and environmental monitoring.

This work was done by Gary W. Hunter and Jennifer C. Xu of Glenn Research Center and Chung-Chiun Liu of Case Western Reserve University. Further information is contained in a TSP (see page 1). *LEW-18674-1*

Inquiries concerning rights for the commercial use of this invention should be addressed to NASA Glenn Research Center, Innovative Partnerships Office, Attn: Steven Fedor, Mail Stop 4–8, 21000 Brookpark Road, Cleveland, Ohio 44135. Refer to LEW-18674-1.

Pressure Shell Approach to Integrated Environmental Protection

Lyndon B. Johnson Space Center, Houston, Texas

The next generation of exploration mission human systems will require environmental protection such as radiation protection that is effective and efficient. In order to continue human exploration, habitat systems will require special shells to protect astronauts from hostile environments. The Pressure Shell Approach to integrated environmental (radiation) protection is a multi-layer shell that can be used for multifunctional environmental protection. Self-healing, self-repairing nano technologies and sensors are incorporated into the shell. This shell consists of multiple layers that can be tailored for specific environmental protection needs. Mainly, this innovation focuses on protecting crew from exposure to micrometeorites, thermal, solar flares, and galactic cosmic ray (GCR) radiation.

The Pressure Shell Approach consists of a micrometeoroid and secondary ejecta protection layer; a thin, composite shell placed in between two layers that is non-structural; an open cavity layer that can be filled with water, regolith, or polyethylene foam; a thicker composite shell that is a structural load bearing that is placed between two layers; and a bladder coating on the interior composite shell. This multi-layer shell creates an effective radiation protection system. Most of its layers can be designed with the materials necessary for specific environments. *In situ* materials such as water or regolith can be added to the shell design for supplemental radiation protection.

This work was done by Kriss J. Kennedy of Johnson Space Center. Further information is contained in a TSP (see page 1). MSC-24637-1

Image Quality Indicator for Infrared Inspections

John F. Kennedy Space Center, Florida

The quality of images generated during an infrared thermal inspection depends on many system variables, settings, and parameters to include the focal length setting of the IR camera lens. If any relevant parameter is incorrect or sub-optimal, the resulting IR images will usually exhibit inherent unsharpness and lack of resolution.

Traditional reference standards and image quality indicators (IQIs) are made of representative hardware samples and contain representative flaws of concern. These standards are used to verify that representative flaws can be detected with the current IR system settings. However, these traditional standards do not enable the operator to quantify the quality limitations of the resulting images, i.e. determine the inherent maximum image sensitivity and image resolution. As a result, the operator does not have the ability to optimize the IR inspection system prior to data acquisition.

The innovative IQI described here eliminates this limitation and enables the operator to objectively quantify and optimize the relevant variables of the IR inspection system, resulting in enhanced image quality with consistency and repeatability in the inspection application.

The IR IQI consists of various copper foil features of known sizes that are printed on a dielectric non-conductive board. The significant difference in thermal conductivity between the two materials ensures that each appears with a distinct grayscale or brightness in the resulting IR image. Therefore, the IR image of the IQI exhibits high contrast between the copper features and the underlying dielectric board, which is required to detect the edges of the various copper features.

The copper features consist of individual elements of various shapes and sizes, or of element-pairs of known shapes and sizes and with known spacing between the elements creating the pair. For example, filled copper circles with various diameters can be used as individual elements to quantify the image sensitivity limit. Copper line-pairs of various sizes where the line width is equivalent to the spacing between the lines can be used as element-pairs to quantify the image resolution limit.

This work was done by Eric Burke of the United Space Alliance, Ground Operations Division, for Kennedy Space Center. Further information is contained in a TSP (see page 1). KSC-13484

Micro-Slit Collimators for X-Ray/Gamma-Ray Imaging

Goddard Space Flight Center, Greenbelt, Maryland

A hybrid photochemical-machining process is coupled with precision stack lamination to allow for the fabrication of multiple ultra-high-resolution grids on a single array substrate. In addition, special fixturing and etching techniques have been developed that allow higher-resolution multi-grid collimators to be fabricated.

Building on past work of developing a manufacturing technique for fabricating multi-grid, high-resolution coating modulation collimators for arcsecond and sub-arcsecond x-ray and gamma-ray imaging, the current work reduces the grid pitch by almost a factor of two, down to 22 microns. Additionally, a process was developed for reducing thin, high-Z (tungsten or molybdenum) from the thinnest commercially available foil (25 microns thick) down to ≈10 microns thick using precisely controlled chemical etching.

This work was done by Michael Appleby, Iain Fraser, and Jill Klinger of Mikro Systems Inc. for Goddard Space Flight Center. For further information, contact the Goddard Innovative Partnerships Office at (301) 286-5810. GSC-15628-1

Scatterometer-Calibrated Stability Verification Method

This method can be used in microwave remote sensing, telecommunications, and in reconnaissance and homeland security applications.

NASA's Jet Propulsion Laboratory, Pasadena, California

The requirement for scatterometer-combined transmit-receive gain variation knowledge is typically addressed by sampling a portion of the transmit signal, attenuating it with a known-stable attenuation, and coupling it into the receiver chain. This way, the gain variations of the transmit and receive chains are represented by this loop-back calibration signal, and can be subtracted from the received remote radar echo. Certain challenges are presented by this process, such as transmit and receive components that are outside of this loop-back path and are not included in this calibration, as well as the impracticality for measuring the transmit and receive chains' stability and post fabrication separately,

without the resulting measurement errors from the test set up exceeding the requirement for the flight instrument.

To cover the RF stability design challenge, the portions of the scatterometer that are not calibrated by the loop-back, (e.g., attenuators, switches, diplexers, couplers, and coaxial cables) are tightly thermally controlled, and have been characterized over temperature to contribute less than 0.05 dB of calibration error over worst-case thermal variation. To address the verification challenge, including the components that are not calibrated by the loop-back, a stable fiber optic delay line (FODL) was used to delay the transmitted pulse, and to route it into the receiver. In this way, the internal loop-back signal amplitude variations can be compared to the full transmit/receive external path, while the flight hardware is in the worst-case thermal environment.

The practical delay for implementing the FODL is 100 μs. The scatterometer pulse width is 1 ms so a test mode was incorporated early in the design phase to scale the 1 ms pulse at 100-Hz pulse repetition interval (PRI), by a factor of 18, to be a 55 μs pulse with 556 μs PRI. This scaling maintains the duty cycle, thus maintaining a representative thermal state for the RF components.

The FODL consists of an RF-modulated fiber-optic transmitter, 20 km SMF-28 standard single-mode fiber, and a photodetector. Thermoelectric cooling and insulating packaging are used to achieve high thermal stability of the FODL components. The chassis was insulated with 1-in. (≈2.5-cm) thermal isolation foam. Nylon rods support the Micarta plate, onto which are mounted four 5-km fiber spool boxes. A copper plate heat sink was mounted on top of the fiber boxes (with thermal grease layer) and screwed onto the thermoelectric cooler plate. Another thermal isolation layer in the middle separates the fiber-optics chamber from the RF electronics components, which are also mounted on a copper plate that is screwed onto another thermoelectric cooler.

The scatterometer subsystem's overall stability was successfully verified to be calibratable to within 0.1 dB error in thermal vacuum (TVAC) testing with the fiber-optic delay line, while the scatterometer temperature was ramped from 10 to 30 °C, which is a much larger temperature range than the worst-case expected seasonal variations.

This work was done by Dalia A. McWatters, Craig M. Cheetham, Shouhua Huang, Mark A. Fischman, Anhua J. Chu, and Adam P. Freedman of Caltech for NASA's Jet Propulsion Laboratory. Further information is contained in a TSP (see page 1). NPO-47559

Test Port for Fiber-Optic-Coupled Laser Altimeter

Test port simplifies verification of focal setting and boresight alignment.

Goddard Space Flight Center, Greenbelt, Maryland

A test port designed as part of a fiber-optic-coupled laser altimeter receiver optical system allows for the back-illumination of the optical system for alignment verification, as well as illumination of the detector(s) for testing the receiver electronics and signal-processing algorithms. Measuring the optical alignment of a laser altimeter instrument is difficult after the instrument is fully assembled. The addition of a test port in the receiver aft-optics allows for the back-illumination of the receiver system such that its focal setting and boresight alignment can be easily verified. For a multiple-detector receiver system, the addition of the aft-optics test port offers the added advantage of being able to simultaneously test all the detectors with different signals that simulate the expected operational conditions.

On a laser altimeter instrument (see figure), the aft-optics couple the light from the receiver telescope to the receiver detector(s). Incorporating a beam splitter in the aft-optics design allows for the addition of a test port to back-illuminate the receiver telescope and/or detectors. The aft-optics layout resembles a "T" with the detector on one leg, the receiver telescope input port on the second leg, and the test port on the third leg. The use of a custom beam splitter with 99-percent reflection, 1-percent transmission, and a mirrored roof can send the test port light to the receiver telescope leg as well as the detector leg, without unduly sacrificing the signal from the receiver telescope to the detector.

The ability to test the receiver system alignment, as well as multiple detectors

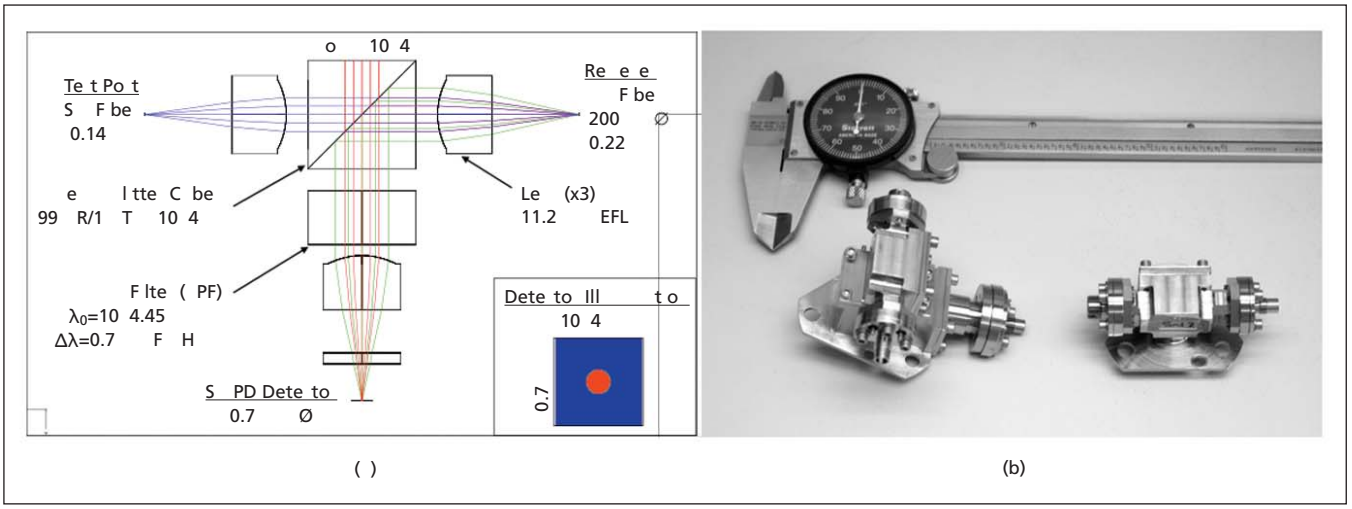

Lunar Orbiter Laser Altimeter (LOLA) Aft-Optics: (a) Optical Layout, (b) Assemblies.

with different signals without the need to disassemble the instrument or connect and reconnect components, is a great advantage to the aft-optics test port. Another benefit is that the receiver telescope aperture is fully back-illuminated by the test port so the receiver telescope focal setting vs. pressure and or temperature can be accurately measured (as compared to schemes where the aperture is only partially illuminated). Fiber-optic coupling the test port also allows for the modularity of testing the receiver detectors with a variety of background and signal laser sources without the need of using complex optical set-ups to optimize the efficiency of each source.

This work was done by Luis Ramos-Izquierdo, V. Stanley Scott, Haris Riris, and John Cavanaugh of Goddard Space Flight Center. For further information, contact the Goddard Innovative Partnerships Office at (301) 286-5810. GCS-15890-1

Phase Retrieval System for Assessing Diamond Turning and Optical Surface Defects

Goddard Space Flight Center, Greenbelt, Maryland

An optical design is presented for a measurement system used to assess the impact of surface errors originating from diamond turning artifacts. Diamond turning artifacts are common by-products of optical surface shaping using the diamond turning process (a diamond-tipped cutting tool used in a lathe configuration).

Assessing and evaluating the errors imparted by diamond turning (including other surface errors attributed to optical manufacturing techniques) can be problematic and generally requires the use of an optical interferometer. Commercial interferometers can be expensive when compared to the simple optical setup developed here, which is used in combination with an image-based sensing technique (phase retrieval). Phase retrieval is a general term used in optics to describe the estimation of optical imperfections or "aberrations."

This turnkey system uses only image-based data and has minimal hardware requirements. The system is straightforward to set up, easy to align, and can provide nanometer accuracy on the measurement of optical surface defects.

This work was done by Bruce Dean, Alex Maldonado, and Matthew Bolcar of the Goddard Space Flight Center. Further information is contained in a TSP (see page 1). GSC-15976-1

Laser Oscillator Incorporating a Wedged Polarization Rotator and a Porro Prism as Cavity Mirror

Goddard Space Flight Center, Greenbelt, Maryland

A laser cavity was designed and implemented by using a wedged polarization rotator and a Porro prism in order to reduce the parts count, and to improve the laser reliability. In this invention, a z-cut quartz polarization rotator is used to compensate the wavelength retardance introduced by the Porro prism. The polarization rotator rotates the polarization of the linear polarized beam with a designed angle that is independent of the orientation of the rotator. This unique property was used to combine the retardance compensation and a Risley prism to a single optical component: a wedged polarization rotator. This greatly simplifies the laser alignment procedure and reduces the number of the laser optical components.

This work was done by Steven Li of Goddard Space Flight Center. Further information is contained in a TSP (see page 1). GSC-15833-1

Generic, Extensible, Configurable Push-Pull Framework for Large-Scale Science Missions

This framework also has been evaluated for data dissemination supporting the National Cancer Institute's early cancer detection research network.

NASA's Jet Propulsion Laboratory, Pasadena, California

The push-pull framework was developed in hopes that an infrastructure would be created that could literally connect to any given remote site, and (given a set of restrictions) download files from that remote site based on those restrictions.

The Cataloging and Archiving Service (CAS) has recently been re-architected and re-factored in its canonical services, including file management, workflow management, and resource management. Additionally, a generic CAS Crawling Framework was built based on motivation from Apache's open-source search engine project called Nutch. Nutch is an Apache effort to provide search engine services (akin to Google), including crawling, parsing, content analysis, and indexing. It has produced several stable software releases, and is currently used in production services at companies such as Yahoo, and at NASA's Planetary Data System.

The CAS Crawling Framework supports many of the Nutch Crawler's generic services, including metadata extraction, crawling, and ingestion. However, one service that was not ported over from Nutch is a generic protocol layer service that allows the Nutch crawler to obtain content using protocol plug-ins that download content using implementations of remote protocols, such as HTTP, FTP, WinNT file system, HTTPS, etc. Such a generic protocol layer would greatly aid in the CAS Crawling Framework, as the layer would allow the framework to generically obtain content (i.e., data products) from remote sites using protocols such as FTP and others. Augmented with this capability, the Orbiting Carbon Observatory (OCO) and NPP (NPOESS Preparatory Project) Sounder PEATE (Product Evaluation and Analysis Tools Elements) would be provided with an infrastructure to support generic FTP-based pull access to remote data products, obviating the need for any specialized software outside of the context of their existing process control systems.

This extensible configurable framework was created in Java, and allows the use of different underlying communication middleware (at present, both XML-RPC, and RMI). In addition, the framework is entirely suitable in a multi-mission environment and is supporting both NPP Sounder PEATE and the OCO Mission. Both systems involve tasks such as high-throughput job processing, terabyte-scale data management, and science computing facilities. NPP Sounder PEATE is already using the push-pull framework to accept hundreds of gigabytes of IASI (infrared atmospheric sounding interferometer) data, and is in preparation to accept CRIMS (Cross-track Infrared Microwave Sounding Suite) data. OCO will leverage the framework to download MODIS, CloudSat, and other ancillary data products for use in the high-performance Level 2 Science Algorithm.

The National Cancer Institute is also evaluating the framework for use in sharing and disseminating cancer research data through its Early Detection Research Network (EDRN).

This work was done by Brian M. Foster, Albert Y. Chang, Dana J. Freeborn, Daniel J. Crichton, David M. Woollard, and Chris A. Mattmann of Caltech for NASA's Jet Propulsion Laboratory. For more information, contact iaoffice@jpl.nasa.gov.

The software used in this innovation is available for commercial licensing. Please contact Daniel Broderick of the California Institute of Technology at danielb@caltech.edu. Refer to NPO-46185.

Dynamic Loads Generation for Multi-Point Vibration Excitation Problems

Marshall Space Flight Center, Alabama

A random-force method has been developed to predict dynamic loads produced by rocket-engine random vibrations for new rocket-engine designs. The method develops random forces at multiple excitation points based on random vibration environments scaled from accelerometer data obtained during hot-fire tests of existing rocket engines. This random-force method applies random forces to the model and creates expected dynamic response in a manner that simulates the way the operating engine applies self-generated random vibration forces (random pressure acting on an area) with the resulting responses that we measure with accelerometers. This innovation includes the methodology (implementation sequence), the computer code, two methods to generate the random-force vibration spectra, and two methods to reduce some of the inherent conservatism in the dynamic loads.

This methodology would be implemented to generate the random-force spectra at excitation nodes without requiring the use of artificial boundary conditions in a finite element model. More accurate random dynamic loads than those predicted by current industry methods can then be generated using the random force spectra. The scaling

method used to develop the initial power spectral density (PSD) environments for deriving the random forces for the rocket engine case is based on the Barrett Criteria developed at Marshall Space Flight Center in 1963. This invention approach can be applied in the aerospace, automotive, and other industries to obtain reliable dynamic loads and responses from a finite element model for any structure subject to multi-point random vibration excitations.

This work was done by Lawrence Shen of Pratt & Whitney Rocketdyne for Marshall Space Flight Center. For more information, contact Sammy Nabors, MSFC Commercialization Assistance Lead, at sammy.a.nabors@nasa.gov. Refer to MFS-32714-1.

Optimal Control Via Self-Generated Stochasticity

NASA's Jet Propulsion Laboratory, Pasadena, California

The problem of global maxima of functionals has been examined. Mathematical roots of local maxima are the same as those for a much simpler problem of finding global maximum of a multi-dimensional function. The second problem is instability — even if an optimal trajectory is found, there is no guarantee that it is stable. As a result, a fundamentally new approach is introduced to optimal control based upon two new ideas.

The first idea is to represent the functional to be maximized as a limit of a probability density governed by the appropriately selected Liouville equation. Then, the corresponding ordinary differential equations (ODEs) become stochastic, and that sample of the solution that has the largest value will have the highest probability to appear in ODE simulation. The main advantages of the stochastic approach are that it is not sensitive to local maxima, the function to be maximized must be only integrable but not necessarily differentiable, and global equality and inequality constraints do not cause any significant obstacles.

The second idea is to remove possible instability of the optimal solution by equipping the control system with a self-stabilizing device.

The applications of the proposed methodology will optimize the performance of NASA spacecraft, as well as robot performance.

This work was done by Michail Zak of Caltech for NASA's Jet Propulsion Laboratory. For more information, contact iaoffice@jpl.nasa.gov. NPO-46923

Space-Time Localization of Plasma Turbulence Using Multiple Spacecraft Radio Links

This technology has applications in forecasting adverse effects on satellites.

NASA's Jet Propulsion Laboratory, Pasadena, California

Space weather is described as the variability of solar wind plasma that can disturb satellites and systems and affect human space exploration. Accurate prediction requires information of the heliosphere inside the orbit of the Earth. However, for predictions using remote sensing, one needs not only plane-of-sky position but also range information — the third spatial dimension — to show the distance to the plasma disturbances and thus when they might propagate or co-rotate to create disturbances at the orbit of the Earth. Appropriately processed radio signals from spacecraft having communications lines-of-sight passing through the inner heliosphere can be used for this space-time localization of plasma disturbances.

The solar plasma has an electron density- and radio-wavelength-dependent index of refraction. An approximately monochromatic wave propagating through a thin layer of plasma turbulence causes a geometrical-optics phase shift proportional to the electron density at the point of passage, the radio wavelength, and the thickness of the layer. This phase shift is the same for a wave propagating either "up" or "down" through the layer at the point of passage. This attribute can be used for space-time localization of plasma irregularities.

The transfer function of plasma irregularities to the observed time series depends on the Doppler tracking "mode." When spacecraft observations are in the two-way mode (downlink radio signal phase-locked to an uplink radio transmission), plasma fluctuations have a "two-pulse" response in the Doppler. In the two-way mode, the Doppler time series $y_2(t)$ is the difference between the frequency of the downlink signal received and the frequency of a ground reference oscillator. A plasma blob localized at a distance x along the line of sight perturbs the phase on both the up and down link, giving rise to two events in the two-way tracking time series separated by a time lag depending the blob's distance from the Earth: $T_2 - 2x/c$, where T_2 is the two-way time-of-flight of radio waves to/from the spacecraft and c is the speed of light.

In some tracking situations, more information is available. For example, with the 5-link Cassini radio system, the plasma contribution to the up and down links, $y_{up}(t)$ and $y_{dn}(t)$, can be computed separately. The times series $y_{up}(t)$ and $y_{dn}(t)$ respond to a localized plasma blob with one event in each time series. These events are also separated in time by $T_2 - 2x/c$. By cross-correlating the up and down link Doppler time series, the time separation of the plasma events can be measured and hence the plasma blob's distance from the Earth determined. Since the plane-of-sky position is known, this technique allows localization of plasma events in time and three space dimensions.

This work was done by John W. Armstrong and Frank B. Estabrook of Caltech for NASA's Jet Propulsion Laboratory. For more information, contact iaoffice@jpl.nasa.gov. NPO-46952

Surface Contact Model for Comets and Asteroids

NASA's Jet Propulsion Laboratory, Pasadena, California

A contact force model was developed for use in touch and go (TAG) surface sampling simulations on small celestial bodies such as comets and asteroids. In TAG scenarios, a spacecraft descending toward the surface of a small body comes into contact with the surface for a short duration of time, collects material samples with a sampler device, and then ascends to leave the surface. The surface contact required 6-DOF (degrees of freedom) dynamics models due to coupling of the attitude and translation dynamics during the contact.

The model described here is for contact scenarios that utilize a rotating brush wheel sampler (BWS) to collect surface material. The model includes stiffness and damping of the surface material during BWS vertical motion, lateral friction from the BWS dragging across the surface, and lateral shear from the rotating BWS scooping the surface material.

This model is useful for any mission to asteroids or comets that incorporates surface sampling operations.

This work was done by Lars James C. Blackmore, Brian P. Trease, Behcet Acikmese, Milan Mandic, and John M. Carson of Caltech for NASA's Jet Propulsion Laboratory. Further information is contained in a TSP (see page 1). NPO-47194

Books & Reports

Dust Mitigation Vehicle

A document describes the development and demonstration of an apparatus, called a "dust mitigation vehicle," for reducing the amount of free dust on the surface of the Moon. The dust mitigation vehicle would be used to pave surfaces on the Moon to prevent the dust from levitating or adhering to surfaces.

The basic principle of operation of these apparatuses is to use a lens or a dish mirror to concentrate solar thermal radiation onto a small spot to heat lunar regolith. In the case of the prototype dust mitigation vehicle, a Fresnel lens was used to heat a surface layer of regolith sufficiently to sinter or melt dust grains into a solid mass. The prototype vehicle has demonstrated paving rates up to 1.8 m^2 per day. The proposed flight design of the dust mitigation vehicle is also described.

This work was done by Eric H. Cardiff of Goddard Space Flight Center. Further information is contained in a TSP (see page 1). GSC-15488-1

Optical Coating Performance for Heat Reflectors of the JWST-ISIM Electronic Component

A document discusses a thermal radiator design consisting of lightweight composite materials and low-emittance metal coatings for use on the James Webb Space Telescope (JWST) structure. The structure will have a Thermal Subsystem unit to provide passive cooling to the Integrated Science Instrument Module (ISIM) control electronics. The ISIM, in the JWST observatory, is the platform that provides the mounting surfaces for the instrument control electronics. Dissipating the control electronic generated-heat away from JWST is of paramount importance so that the spacecraft's own heat does not interfere with the infrared-light gathering of distant cosmic sources.

The need to have lateral control in the emission direction of the IEC (ISIM Electronics Compartment) radiators led to the development of a directional baffle design that uses multiple curved mirrorlike surfaces. This concept started out from the so-called Winston non-imaging optical concentrators that use opposing parabolic reflector surfaces, where each parabola has its focus at the opposite edge of the exit aperture. For this reason they are often known as compound parabolic concentrators or CPCs.

This radiator system with the circular section was chosen for the IEC reflectors because it offers two advantages over other designs. The first is that the area of the reflector strips for a given radiator area is less, which results in a lower mass baffle assembly. Secondly, the fraction of energy emitted by the radiator strips and subsequently reflected by the baffle is less. These fewer reflections reduced the amount of energy that is absorbed and eventually re-emitted, typically in a direction outside the design emission range angle.

A baffle frame holds the mirrors in position above a radiator panel on the IEC. Together, these will direct the majority of the heat from the IEC above the sunshield away towards empty space.

This work was done by Robert A. Rashford, Charles M. Perrygo, Matthew B. Garrison, Bryant K. White, Felix T. Threat, Manuel A. Quijada, James W. Jeans, Frank K. Huber, Robert R. Bousquet, and Dave Shaw of Goddard Space Flight Center. Further information is contained in a TSP (see page 1). GSC-15823-1

SpaceCube Demonstration Platform

A document discusses how the HST SM4 SpaceCube flight spare was modified to create an experiment called the SpaceCube Demonstration Platform (SC DP) for use on the MISSE7 Space Station payload (in collaboration with NRL). It is designed to serve as an on-orbit platform for demonstrating advanced fault tolerance technologies. A simple C&DH (command and data handling) system was developed for the Virtex4 FPGAs (field programmable gate arrays). Both Virtex4s on each SpaceCube run the same program, and both receive incoming telemetry. The rad-hard service FPGA performs simple error checking to verify that the incoming telemetry is valid. The SpaceCube framework was modified to allow for new program files to be sent from the ground, to be stored on the SpaceCube, and to be executed through ground commands. Each SpaceCube Virtex4 FPGA has resources set aside for experiments that are functionally isolated from the C&DH system. The experiments communicate to the C&DH system through a set of dual port memories, and this area is where the fault-tolerance experiments are executed.

With the use of Xilinx commercial Virtex4 FX60 FPGAs, the fault tolerant framework allows the system to recover from radiation upsets that occur in the rad-soft parts (Virtex4 FPGA logic, embedded PPCs in Virtex4 FPGAs, SDRAM and Flash), the C&DH system that runs simultaneously on both Virtex4 FPGAs that uses a robust telemetry packet structure, checksums, and the rad-hard service FPGA to validate incoming telemetry. The ability to be reconfigured from the ground while in orbit is a novel benefit, as well as is the onboard compression capabilities that allow compressed files from the ground to be uploaded to the SpaceCube.

This work was done by Daniel Espinosa, Jeffrey Hosler, Alessandro Geist, David Petrick, Manuel Buenfil, Gary Crum, and Tom Flatley for Goddard Space Flight Center. Further information is contained in a TSP (see page 1). GSC-15953-1

Aperture Mask for Unambiguous Parity Determination in Long Wavelength Imagers

A document discusses a new parity pupil mask design that allows users to unambiguously determine the image space coordinate system of all the James Webb Space Telescope (JWST) science instruments by using two out-of-focus images. This is an improvement over existing mask designs that could not completely eliminate the coordinate system parity ambiguity at a wavelength of 5.6 microns. To mitigate the problem of how the presence of diffraction artifacts can obscure the pupil mask detail, this innovation has been created with specifically designed edge features so that the image space coordinate system parity can be determined in the presence of diffraction, even at long wavelengths.

This work was done by Brent Bos for Goddard Space Flight Center. Further information is contained in a TSP (see page 1). GSC-15956-1

Spaceflight Ka-Band High-Rate Radiation-Hard Modulator

A document discusses the creation of a Ka-band modulator developed specifically for the NASA/GSFC Solar Dynamics Observatory (SDO). This flight design consists of a high-bandwidth, Quadriphase Shift Keying (QPSK) vector modulator with radiation-hardened, high-rate driver circuitry that receives I and Q channel data. The radiation-hard design enables SDO's Ka-band communications downlink system to transmit 130 Mbps (300 Msps after data encoding) of science instrument data to the ground system continuously throughout the mission's minimum life of five years. The low error vector magnitude (EVM) of the modulator lowers the implementation loss of the transmitter in which it is used, thereby increasing the overall communication system link margin.

The modulator comprises a component within the SDO transmitter, and meets the following specifications over a 0 to 40 °C operational temperature range: QPSK/OQPSK modulator, 300-Msps symbol rate, 26.5-GHz center frequency, error vector magnitude ≤10 percent rms, and compliance with the NTIA (National Telecommunications and Information Administration) spectral mask.

This work was done by Jeffery M. Jaso of Goddard Space Flight Center. Further information is contained in a TSP (see page 1). GSC-15217-1

Enabling Disabled Persons To Gain Access to Digital Media

A report describes the first phase in an effort to enhance the NaviGaze software to enable profoundly disabled persons to operate computers. (Running on a Windows-based computer equipped with a video camera aimed at the user's head, the original NaviGaze software processes the user's head movements and eye blinks into cursor movements and mouse clicks to enable hands-free control of the computer.) To accommodate large variations in movement capabilities among disabled individuals, one of the enhancements was the addition of a graphical user interface for selection of parameters that affect the way the software interacts with the computer and tracks the user's movements. Tracking algorithms were improved to reduce sensitivity to rotations and reduce the likelihood of tracking the wrong features. Visual feedback to the user was improved to provide an indication of the state of the computer system. It was found that users can quickly learn to use the enhanced software, performing single clicks, double clicks, and drags within minutes of first use. Available programs that could increase the usability of NaviGaze were identified. One of these enables entry of text by using NaviGaze as a mouse to select keys on a virtual keyboard.

This work was done by Glenn Beach and Ryan O'Grady of Cybernet Systems Corp. for Goddard Space Flight Center. Further information is contained in a TSP (see page 1). GSC-14930-1

Cytometer on a Chip

Analyses could be performed rapidly in compact instruments using disposable chips.

Lyndon B. Johnson Space Center, Houston, TX

A cytometer now under development exploits spatial sorting of sampled cells on a microarray chip followed by use of grating-coupled surface-plasmon-resonance imaging (GCSPRI) to detect the sorted cells. This cytometer on a chip is a prototype of contemplated future miniature cytometers that would be suitable for rapidly identifying pathogens and other cells of interest in both field and laboratory applications and that would be attractive as alternatives to conventional flow cytometers.

The basic principle of operation of a conventional flow cytometer requires fluorescent labeling of sampled cells, stringent optical alignment of a laser beam with a narrow orifice, and flow of the cells through the orifice, which is subject to clogging. In contrast, the principle of operation of the present cytometer on a chip does not require fluorescent labeling of cells, stringent optical alignment, or flow through a narrow orifice. The basic principle of operation of the cytometer on a chip also reduces the complexity, mass, and power of the associated laser and detection systems, relative to those needed in conventional flow cytometry.

Instead of making cells flow in single file through a narrow flow orifice for sequential interrogation as in conventional flow cytometry, a liquid containing suspended sampled cells is made to flow over the front surface of a microarray chip on which there are many capture spots. Each capture spot is coated with a thin (≈50-nm) layer of gold that is, in turn, coated with antibodies that bind to cell-surface molecules characteristic of the cell species of interest. The multiplicity of capture spots makes it possible to perform rapid, massively parallel analysis of a large cell population.

The binding of cells to each capture spot gives rise to a minute change in the index of refraction at the surface of the chip. This change in the index of refraction is what is sensed in GCSPRI, as described briefly below. The identities of the various species in a sample of cells is spatially encoded in the chip by the pattern of capture spots. The number of cells of a particular species is determined from the magnitude of the GCSPRI signal from that spot.

GCSPRI as used here can be summarized as follows: The cytometer chip is fabricated with a diffraction grating on its front surface. The chip is illuminated with a light emitting diode (LED) from the front. By proper choice of grating parameters and of the wavelength and the angle of incidence of a laser beam, laser light can be made to be coupled into an electromagnetic mode that resonates with surface plasmons and thus couples light into surface plasmons. Coupling of light into a surface plasmon at a given location reduces the amount of incident light reflected from that location. A change in the index of refraction at the surface of a capture spot gives rise to a change in the resonance condition. Depending on the specific design, the change in the index of refraction could manifest itself as a brightening or darkening, a change in the wavelength needed to excite the plasmon at a given angle of incidence, or a change in the angle of incidence needed to excite the plasmon at a given wavelength.

Whereas a multiwavelength laser system with multichannel detection would be needed to detect multiple species in conventional flow cytometry, it suffices to use an LED and a single detector channel in the GCSPRI approach: this contributes significantly to reductions in cost, complexity, size, mass, and power. GCSPRI cytometer chips could be made of plastic and could be mass-produced cheaply by use of molding and other methods adopted from the manufacture of digital video disks. These methods are amenable to a high degree of miniaturization: such additional features as fluidic channels, reaction chambers, and fluid-coupling ports could readily be incorporated into the chips, without incurring substantial additional costs.

This work was done by Salvador M. Fernandez of Ciencia, Inc., for Johnson Space Center. Further information is contained in a TSP (see page 1).

In accordance with Public Law 96-517, the contractor has elected to retain title to this invention. Inquiries concerning rights for its commercial use should be addressed to:

Dr. Salvador M. Fernandez, President
Ciencia, Inc.
111 Roberts Street, Suite K
East Hartford, CT. 06108
Phone No.:(860) 528-9737
Fax No.:(860) 528-5658

Refer to MSC-23711-1/4224-1, volume and number of this Medical Design Briefs *issue, and the page number.*

Principles, Techniques, and Applications of Tissue Microfluidics

This technique can be used in the diagnosis of diseases such as cancer.

NASA's Jet Propulsion Laboratory, Pasadena, CA

The principle of tissue microfluidics and its resultant techniques has been applied to cell analysis. Building microfluidics to suit a particular tissue sample would allow the rapid, reliable, inexpensive, highly parallelized, selective extraction of chosen regions of tissue for purposes of further biochemical analysis. Furthermore, the applicability of the techniques ranges beyond the described pathology application. For example, they would also allow the posing and success-

ful answering of new sets of questions in many areas of fundamental research.

The proposed integration of microfluidic techniques and tissue slice samples is called "tissue microfluidics" because it molds the microfluidic architectures in accordance with each particular structure of each specific tissue sample. Thus, microfluidics can be built around the tissues, following the tissue structure, or alternatively, the microfluidics can be adapted to the specific geometry of particular tissues. By contrast, the traditional approach is that microfluidic devices are structured in accordance with engineering considerations, while the biological components in applied devices are forced to comply with these engineering presets.

The proposed principles represent a paradigm shift in microfluidic technology in three important ways:

- Microfluidic devices are to be directly integrated with, onto, or around tissue samples, in contrast to the conventional method of off-chip sample extraction followed by sample insertion in microfluidic devices.
- Architectural and operational principles of microfluidic devices are to be subordinated to suit specific tissue structure and needs, in contrast to the conventional method of building devices according to fluidic function alone and without regard to tissue structure.
- Sample acquisition from tissue is to be performed on-chip and is to be integrated with the diagnostic measurement within the same device, in contrast to the conventional method of off-chip sample prep and subsequent insertion into a diagnostic device. A more advanced form of tissue integration with microfluidics is tissue encapsulation, wherein the sample is completely encapsulated within a microfluidic device, to allow for full surface access.

The immediate applications of these approaches lie with diagnostics of tissue slices and biopsy samples — e.g. for cancer — but the approaches would also be very useful in comparative genomics and other areas of fundamental research involving heterogeneous tissue samples.

The approach advocates and utilizes the bottom-up customization of microfluidic architectures to biosamples, in contrast to the traditional top-down approach of building the architectures first and then putting the biosamples inside. Further, as particular embodiments of the above principle, novel techniques of sub-sample selection and isolation are presented. These techniques would have wide applicability in fundamental research and biomedical diagnostics.

In particular, an *in situ* microfluidic technique of single-cell isolation, or multiple single-cell isolations, is described, and is performed upon tissue sections attached to pathology glass slides. The technique combines the advantages of preserving the architectural integrity of the tissue section while allowing flexibility and precision of cell selection, rapid prototyping, and enhanced sample purity, while benefiting from the experience of the pathologist in the selection process. The result is a system that would allow the rapid and reliable biochemical analysis and diagnosis of pathologic processes with sensitivity extended down to the level of even a single cell, with high levels of confidence in the diagnostic determination.

These techniques would allow the extraction of cells and cell nuclei chosen for their potentially pathologic origin, e.g. cancer. The chief advantages of the proposed methods are their speed, ease, reliability, and capacity to select individual cells from a tissue slice population with a higher degree of purity and specificity. The result is the extracted DNA can be biochemically analyzed with a higher degree of diagnostic accuracy, as the isolated sub-sample would not be diluted by unwanted material from the ambient tissue. In comparison to other techniques, the proposed methods would combine high specificity with high speed.

This work was done by Lawrence A. Wade of Caltech and Emil P. Kartalov, Darryl Shibata, and Clive Taylor of the University of Southern California for NASA's Jet Propulsion Laboratory. Further information is contained in a TSP (see page 1).

Refer to NPO-47561, volume and number of this Medical Design Briefs *issue, and the page number.*

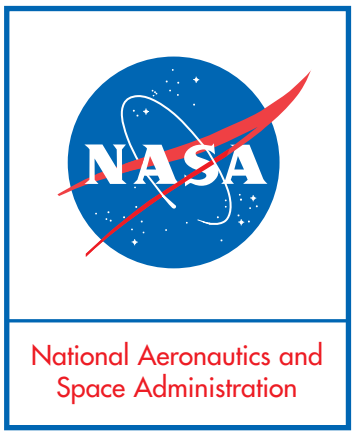
NASA
National Aeronautics and
Space Administration